Cell Stress and Chaperones (2021) 26:77–90
https://doi.org/10.1007/s12192-020-01157-2

ORIGINAL PAPER

MiR-17-5p-mediated endoplasmic reticulum stress promotes acute myocardial ischemia injury through targeting Tsg101

Linlin Zhao[1] · Shan Jiang[2] · Naishi Wu[3] · Enyi Shi[4] · Lin Yang[5] · Qiang Li[1]

Received: 17 April 2020 / Revised: 18 August 2020 / Accepted: 23 August 2020 / Published online: 8 September 2020

Abstract

Cardiovascular diseases are the leading cause of death globally, among which acute myocardial infarction (AMI) frequently occurs in the heart and proceeds from myocardium ischemia and endoplasmic reticulum (ER) stress-induced cell death. Numerous studies on miRNAs indicated their potential as diagnostic biomarkers and treatment targets for heart diseases. Our study investigated the role of miR-17-5p and its regulatory mechanisms during AMI. Echocardiography, MTT, flow cytometry assay, evaluation of caspase-3 and lactate dehydrogenase (LDH) activity were conducted to assess cell viability, apoptosis in an MI/R mice model, and an H_2O_2-induced H9c2 hypoxia cell model, respectively. The expression levels of ER stress response-related biomarkers were detected using qRT-PCR, IHC, and western blotting assays. The binding site of miR-17-5p on Tsg101 mRNA was determined by bioinformatic prediction and luciferase reporter assay. The expression levels of miR-17-5p were notably elevated in MI/R mice and hypoxia cell models, accompanied by enhanced cell apoptosis. Inhibition of miR-17-5p led to decreased apoptosis related to ER stress response in the hypoxia model, which could be counteracted by knockdown of Tsg101 (tumor susceptibility gene 101). Transfection with miR-17-5p mimics downregulated the expression of Tsg101 in H9c2 cells. Luciferase assay demonstrated the binding between miR-17-5p and Tsg101. Moreover, 4-PBA, the inhibitor of the ER stress response, abolished shTsg101 elevated apoptosis in hypoxic H9c2 cells. Our findings investigated the pro-apoptotic role of miR-17-5p during MI/R, disclosed the specific mechanism of miR-17-5p/Tsg101 regulatory axis in ER stress-induced myocardium injury and cardiomyocytes apoptosis, and presented a promising diagnostic biomarker and potential target for therapy of AMI.

Keywords AMI · Hypoxia · Apoptosis · ER stress · miR-17-5p · Tsg101

Introduction

Cardiovascular disease, which is closely related with acute myocardial ischemia (AMI) (World Health Organization (WHO); cardiovascular diseases (CVDs) 2017), is the leading cause of morbidity and mortality worldwide. Numerous studies have indicated that myocardial ischemia initiates a cell apoptosis cascade and leads to further heart failure (Lazou et al. 2006; McCully et al. 2004). Upon ischemia, blood supply to the heart is blocked, causing reduced oxygen supply as well as a massive accumulation of metabolites in cardiomyocytes, leading to increased mechanical stress. For example, the accumulated mitochondrial respiration substrate provides excess reactive oxygen species (ROS) and ATP, leading to hyperactivation of calcium uptake and mitochondrial permeability transition pore (MPTP) that causes ATP depletion in mitochondria, until finally cardiomyocytes undergo uncontrolled death (Chouchani et al. 2014; Harisseh et al. 2019; Rodriguez-Sinovas et al. 2007). In addition, oxidative stress, calcium load alteration, and

✉ Qiang Li
qiangliroll@163.com

[1] Department of Cardiac Surgery, The People's Hospital of Liaoning Province, No.33 Wenyi Road, Shenhe District, Shenyang 110016, Liaoning, People's Republic of China

[2] Department of Respiration, Shengjing Hospital of China Medical University, Shenyang 110000, Liaoning, People's Republic of China

[3] Department of Cardiac Surgery, The Second Affiliated Hospital of Harbin Medical University, Harbin 150001, Heilongjiang, People's Republic of China

[4] Department of Cardiac Surgery, The First Hospital of China Medical University, Shenyang 110001, Liaoning, People's Republic of China

[5] Department of Cardiovascular Medicine, The People's Hospital of Liaoning Province, Shenyang 110016, Liaoning, People's Republic of China

accumulated protein synthesis in endoplasmic reticulum (ER) are also major causes of cardiomyocytes death during AMI (Choy et al. 2018).

ER is the critical membrane organelle in cells and exerts assembling, folding, and surveillance of secretory and transmembrane proteins, meanwhile working with mitochondria to maintain Ca + homeostasis (Groenendyk et al. 2010). Hence, the stability of ER is pivotal for normal physiological functions. Nevertheless, the abnormal cellular conditions under ischemia induce unfolded and misfolded proteins stacking in ER and disturb ER function, resulting in ER stress (Glembotski 2007). At the early stage of ER stress stimulation, the unfolded protein response (UPR) is activated to decrease translation, expands folding capacity, and even starts protein degradation to alleviate ER stress. These reactions are mainly associated with three transmembrane signaling pathways, including the protein kinase RNA-like endoplasmic reticulum kinase (PERK), inositol-requiring protein 1α (IRE1α), and activating transcription factor 6 (ATF6) (Walter and Ron 2011; Wang and Kaufman 2016). The chaperone binding immunoglobulin protein (BiP) is also regarded as a critical factor involved in these processes (Cunard 2015). However, if stress persists, apoptosis would be initiated, characterized by enhanced transcription induction by CHOP (C/EBP homologous protein). CHOP was indicated to be notably associated with apoptosis, typically by activation of caspase-12-associated apoptosis signaling (Miyazaki et al. 2011; Rao et al. 2004). Additionally, CHOP-dependent calcium signaling pathway stimulates apoptosis signaling including Fas death receptor and JNK pathway (Nakagawa et al. 2000; Urano et al. 2000). These fundamental researches render ER stress response a critical target for the prediction and diagnosis of cardiovascular diseases. It is equally important to explore regulatory factors regulating ER stress myocardial ischemia.

MicroRNAs (miRNAs) are principle members of noncoding RNAs, defined as the highly conserved short RNAs with a length of 21–25 nucleotides, and do not translate to proteins (Karbasforooshan et al. 2018). In recent decades, the functions of miRNAs have been widely studied in various diseases, especially in cancer and cardiovascular diseases (Wang et al. 2010, 2019b). MiR-17-5p was reported to exert a diverse function in different cancer types. In thyroid cancer cells, miR-17-5p behaves as an oncogenic factor by downregulating the tumor suppressor Rb1 (Takakura et al. 2008). However, miR-17-5p was revealed to target oncogenes to exert a tumor-suppressive function in breast cancer (Zhang et al. 2007). Studies on cardiovascular diseases demonstrated that administration of miR-17-5p inhibitor improved the cardiac function after AMI (Yang et al. 2018). Nevertheless, the regulatory mechanism of miR-17-5p in myocardial ischemia is yet to be determined.

Tsg101 (tumor susceptibility gene 101) is a functional regulator widely studied in tumors, originally identified as a tumor suppressor while also shown to exert diverse effects in different diseases (Cheng and Cohen 2007; Goff et al. 2003; Sai et al. 2015; Xu and Zheng 2019). However, it is unclear whether Tsg101 affected the progression of AMI. In this study, we evaluated the role of miR-17-5p in ER stress-related cardiomyocytes death under AMI and investigated the role of miR-17-5p/Tsg101 regulatory axis. Our research may provide a novel prospect for the diagnosis and prognosis of AMI.

Materials and methods

Animal feeding

All animal experiments in this study were approved by the standards of Care and Use enacted by Laboratory Animals of the People's Hospital of Liaoning Province. Male C57BL/6 mice which fit specific pathogen-free standards were purchased from Wei Tong Li Hua Company (Beijing, China). The mice were 8 weeks old and weighed around 25 g. The mice were housed in a pathogen-free and ventilated environment at a temperature of about 25 °C with a circadian rhythm of 12 h and fed with sufficient clean water and food. The mice were randomly divided into indicated groups in corresponding experiments.

Myocardial ischemia/reperfusion model

For the myocardial ischemia/reperfusion operation (MI/R group), the mice were initially anesthetized with an injection of sodium pentobarbital at a dose of 30 mg/kg and fixed on an operating heating table at 36–37 °C. The limbs of the mice were connected to electrocardiogram (ECG) for monitoring by electrocardiogram. The left anterior descending (LAD) coronary artery was ligated with 6-0 silk suture. The successful occlusion was indicated by a typical ST segment elevation and successful refusion marked by a recovered T segment. The blood occlusion was administrated for 30 min, and then the blood supplement was restored. The mice in the sham group received a similar operation with no LAD occlusion. The cardiac function was measured by echocardiography 3 days after MI; then the mice were euthanized, and the heart tissues were resected for other experiments.

MiRNA and 4-PBA treatment

For evaluation of miR-17-5p function in a mice MI/R model, miR-17-5p mimic was designed and modified with a methylation and cholesterol package by RiboBio company (Guangzhou, China) to ensure its stability and function in

mice experiments. The injection of miR-17-5p at a dose of 200 nmol/kg dissolved in 60-μL 0.9% saline was performed before ischemia occlusion, via inserting a 30-gauge syringe to the left ventricle. The sham group was operated with the same process with the same volume of 0.9% saline containing no miR-17-5p. A 4-PBA treatment was performed by an intraperitoneal injection at a dose of 20 mg/kg/day before injection of miR-17-5p mimics, until the mice were euthanized. The mice from the sham group were injected with saline.

Echocardiographic measurements

Transthoracic echocardiography was administrated 3 days after surgery. The mice were anesthetized and examined using an ultrasound Vevo 707B system of Visual Sonics Company (Toronto, Ontario, Canada), following the manufacturer's instructions. The M-mode was equipped by a 30-MHz frequency for the capture and calculation of left ventricular ejection fraction (EF%) and fractional shortening (FS%).

Immunohistochemical staining assay

The heart tissues were collected from mice after MI/R, washed with PBS, fixed in 4% paraformaldehyde, and embedded with paraffin. The heart infarction area was cut into 4-μm-thick sections. The coronal sections were treated according to the following process: deparaffinization, blocking of endogenous peroxidase by 2% H_2O_2 incubation, improvement of permeability by 0.1% Triton X-100, incubation with 5% BSA, and then incubation with anti-Bip and anti-CHOP primary antibodies (Abcam, MA, USA) overnight in a 4 °C refrigerator. On the next day, after incubation by HRP-labeled secondary antibody at room temperature for 45 min, the slides were visualized by DAB kit (Beyotime, Shanghai, China). The nucleus was stained with hematoxylin. Five random areas of each slide were captured, and the percentage of positive staining was quantified and calculated as histograms.

Terminal deoxynucleotidyl transferase dUTP nick end labeling assay

For cell apoptosis detection of mice heart tissues, the TUNEL assay was performed following the manufacturer's instructions. The slides were captured and calculated the same with IHC staining.

Cell culture and hypoxia-induced apoptosis model

The cardiomyocyte H9c2 cell line was purchased from American Type Culture Collection (Manassas, VA, USA) and maintained in Dulbecco's Modified Eagle's Medium (DMEM, Gibco, Thermo, MA, USA) containing 10% fetal bovine serum (FBS, Gibco), 100-U/mL penicillin, and 100-μg/mL streptomycin in a 37 °C incubator with a humidified atmosphere and 5% CO_2. To construct a hypoxia model to mimic rat myocardial ischemia-induced cell apoptosis, H9c2 cells were cultured to achieve 80–90% confluence, trypsinized, and seeded in 6-well plates at a density of 1×10^5 cells per well. Then, the DMEM medium with H_2O_2 at a concentration of 200 μm was added to each well and incubated for 4 h.

Measurement of myocardial injury marker and caspase-3 activity

Lactate dehydrogenase (LDH) was regarded as a biomarker released by cells subjected to myocardial ischemia. And caspase-3 activation was regarded as a sign of enhanced apoptosis. We detected the levels of LDH and caspase-3 activity by assay kits purchased from Beyotime (Shanghai, China) following the manufacturer's instructions.

Cell transfection

The sequence of Tsg101 was obtained from the PubMed website. The miR-17-5p mimic, miR-17-5p inhibitor and negative control (NC), and shTsg101 were designed and purchased from RiboBio (Guangzhou, China). The sequences of miRNA and shRNA were as follows: miR-17-5p mimic, 5′-CAAAGUGCUUACAGUGCAGGUAG-3′; miR-17-5p inhibitor, 5′-CUACCUGCACUGUAAGCACUUUG-3′; NC, sense, 5′-ACAAAGUUCUGUGAUGCACUGA-3′; anti-sense, 5′-ACAAAGUUCUGUGAUGCACUGA-3′; and shTsg101, 5′-CCTCCAGTTCCGATAATTT-3′. H9c2 cells were seeded in 6-well plates at a density of 1×10^5 cells per well and incubated overnight to achieve monolayer confluence. After starvation with serum-free medium for 12 h, the cells were transfected with corresponding miRNA or shRNA, as was indicated in each experiment, at 50 nmol/L accompanied with Lipofectamine 2000 (Invitrogen, CA, USA) following the manufacturer's instruction. After transfection for 48 h, the cells were subjected to subsequent experiments.

MTT assay

The proliferation ability of H9c2 cells was analyzed via MTT assay. H9c2 cells were digested and plated into 96-well plates with a density of 1×10^3 cells per well and separately treated with H_2O_2 alone, miR-17-5p, shTsg101, or 4-PBA as indicated in each experiment. At the corresponding end time, 20 μL of MTT (5 mg/mL) (Roche, Basel, Switzerland) was added to each well. Then after a 4-h reaction, the culture medium was discarded, and 150 μL of DMSO was added to each well and incubated in a shaker for 15 min. Then, the absorbance value at a wavelength of 490 nm was detected by an absorbance reader.

RNA extraction and real-time PCR

Total RNAs were extracted using TRIzol Reagent (Invitrogen, CA, USA) following the manufacturer's protocols. Then RNAs were reverse transcribed to cDNA by a cDNA synthesis kit (Takara Biotechnology, Japan). Quantitative real-time PCR (qRT-PCR) was performed to detect gene expression via SYBR Green Supermix Kit (BD, USA) following the manufacturer's protocols. GAPDH and small endogenous nucleolar U6 snRNA were used as an internal control for normalization of miRNA and mRNAs, respectively. Gene expression levels were determined via $2^{-\Delta\Delta Ct}$ method. The primers used in this study were as follows: GAPDH (sense, 5′-AAGA AGGTGGTGAAGCAGGC-3′; antisense, 5′-TCCA CCACCCAGTTGCTGTA-3′); U6 sense (5′-CTCG CTTCGGCAGCACA-3′; antisense, 5′-AACG CTTCACGAATTTGCGT-3′); miR-17-5p (sense, 5′-GGCA AAGTGCTTACAGTGC-3′; antisense, 5′-GTGC AGGGTCCGAGG-3′); and Tsg101 (sense, 5′-CCA AATACTTCCTACATGCCA-3′; antisense, 5′-ATCC CTACTGGGACCAACAGT-3′).

Western blotting

After transfection and HR treatments, H9c2 cells were digested and lysed in × 1 ice-cold RIPA lysis buffer (Beyotime, Shanghai, China). The solution was then centrifuged, and the debris was discarded. The protein concentrations were determined by a BCA kit (TaKaRA, Dalian, China). A total of 35-μg protein was separated by 10% SDS-polyacrylamide gel (PAGE) and then transferred to a polyvinylidene difluoride (PVDF) membrane. Then the blots were blocked at room temperature for 1 h by 5% nonfat milk dissolved in 1 × TBST. The blots were then incubated with specific primary antibodies (anti-PERK, 1:1000; anti-p-PERK, 1:1000; anti-Bip, 1:1000; anti-CHOP, 1:1000; anti-cleaved caspase-3, 1:1000; anti-cleaved caspase-12, 1:1000; anti-Tsg101, 1:1000; anti-GAPDH, 1:1000) at 4 °C overnight. Two hours of incubation was conducted at room temperature with the corresponding secondary antibodies. Subsequently, the membranes were visualized by ECL kit (Invitrogen, CA, USA), and the images were captured using gel imaging system (BD, USA). All antibodies were purchased from Abcam (MA, USA) and diluted following the manufacturer's instructions.

Target prediction

The bioinformatic analysis tool Targets Scan (http://www.targetscan.org) was used to predict the binding sites between miRNA-17-5p and Tsg101.

Luciferase reporter gene assay

The sequence of Tsg101 mRNA was obtained from PubMed (https://www.ncbi.nlm.nih.gov/pubmed). A 293T cell line was purchased from American Type Culture Collection (Manassas, VA, USA) and cultured in DMEM medium with 10% FBS. The wild-type complete sequence and mutated binding sites of miR-17-5p complete sequence of Tsg101 were subcloned into the pGL3 vector (Promega, WI, USA) and named as Tsg101-WT and Tsg101-MUT. The 293T cells were co-transfected with the plasmid constructs of Tsg101-WT or Tsg101-MUT and miR-17-5p mimics or NC by Lipofectamine 3000 (Invitrogen, CA, USA) following the manufacturer's instructions. Subsequently, 0.1 μg pRL-TK plasmid was transfected as an internal control. The luciferase activities were measured with a dual luciferase reporter assay kit (Promega, WI, USA) at 48 h after transfection.

Flow cytometry

Flow cytometry was used to check cell apoptosis. H9c2 cells were plated in a 6-well plate and treated with transfection and H_2O_2 and later collected for dual staining with Annexin V-FITC and propidium iodide following the manufacturer's instructions (Beyotime, Shanghai, China). The cells were analyzed with a flow cytometer (C6, BD, USA). The portion of apoptotic cells in the experimental group was compared with that of the control group in each experiment.

Statistical analysis

The data were presented as the means ± standard deviation (SD). Student's t test and one-way ANOVA were used to assess the difference between two groups and multiple groups, respectively. $P < 0.05$ was considered statistically significant.

Results

Cardiac protective function of miR-17-5p inhibitor during MI/R

To determine the role of miR-17-5p played in MI/R, we constructed a C57BL/6 mouse model to mimic the ischemia status and a hypoxia H2c9 cell model to induce cardiomyocyte cell apoptosis. The results showed that the expression levels of miR-17-5p were significantly elevated ($p < 0.05$) in the peri-infarction area on the first and third days after MI/R (Fig. 1a). In the H_2O_2-induced hypoxia cell model, similar results were obtained showing that miR-17-5p was markedly upregulated ($p < 0.01$) after hypoxia (Fig. 1b). Thus, we speculated that miR-17-5p may promote the cell injury induced by MI/R injury. We performed miR-17-5p inhibition in an in vivo

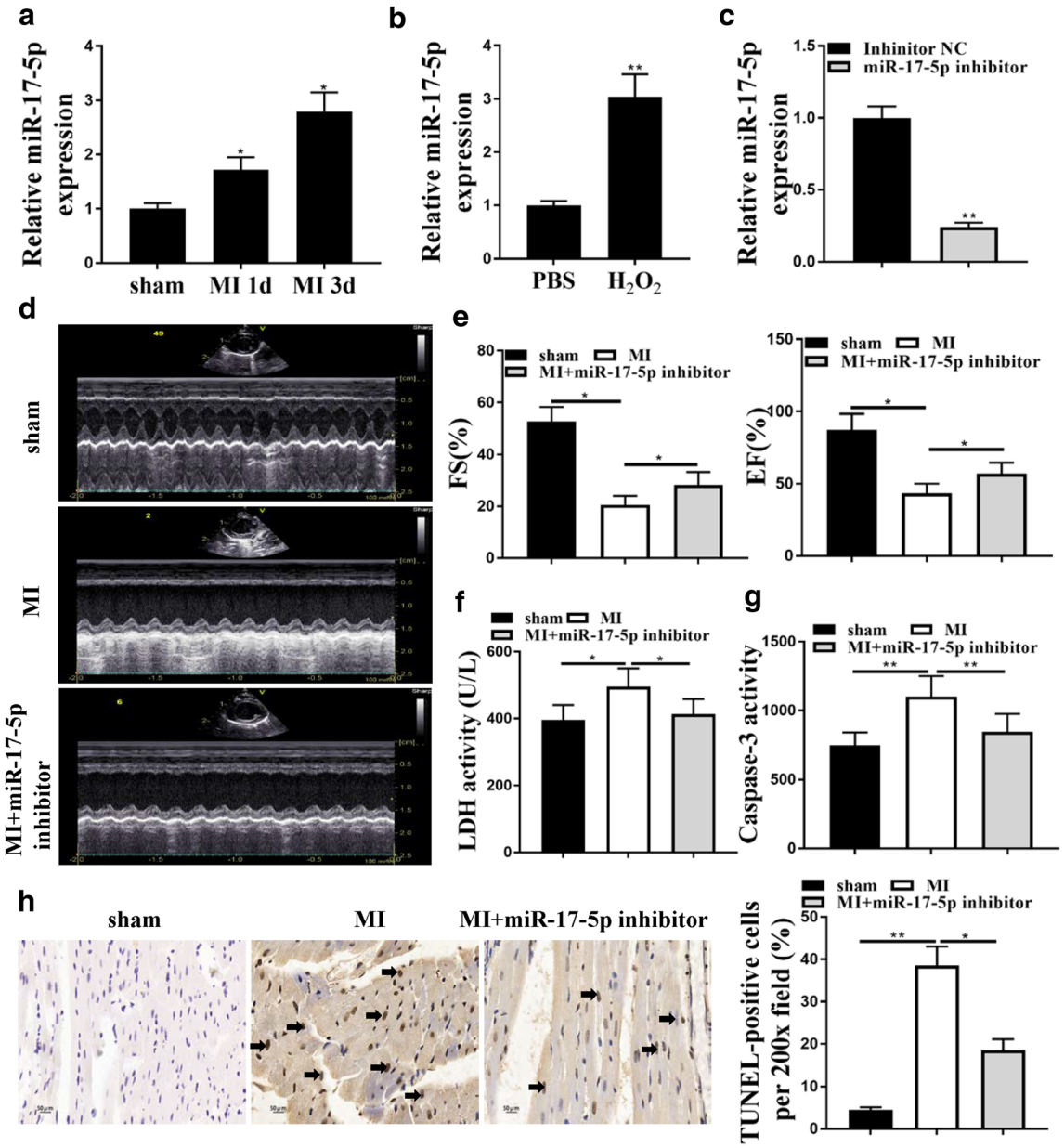

Fig. 1 MiR-17-5p inhibition improves MI/R-induced injury. **a** Elevated level of miR-17-5p in mice heart tissue was detected by qRT-PCR after MI/R. **b** MiR-17-5p detection by qRT-PCR in H9c2 cells after H_2O_2 treatment for 4 h. **c** Level of miR-17-5p detected by qRT-PCR after injection of miR-17-5p inhibitor in mice left ventricular chamber. **d–e** Echocardiography examination of FE and EF after MI/R and miR-17-5p inhibition. **f–g** Serum level of LDH (**f**) and quantification of caspase-3 (**g**) in myocardium by kits. **h** Evaluation of apoptosis in mice hearts after MI/R and miR-17-5p inhibition by TUNEL assay and quantification shown in diagram. Black arrow, positive staining of apoptotic cells. Five random sections were captured and quantified for each sample. Three independent experiments were repeated, $^{*}P < 0.05$, $^{**}P < 0.01$ vs. sham or PBS

experiment by injecting miR-17-5p inhibitor into the left ventricular chamber of mice followed by MI/R for 3 days, and the altered heart injury was evaluated. As shown in Fig. 1c, the expression of miR-17-5p was significantly inhibited ($p < 0.01$) in heart tissue after injection, which indicated the efficacy of the miR-17-5p inhibitor. The echocardiography examination indicated that EF and FS were both significantly decreased ($p < 0.05$) in MI/R hearts compared with that in the sham group and administration of miR-17-5p inhibitor significantly attenuated ($p < 0.05$) the impact (Fig. 1d and e). The detection of myocardial death biomarker LDH in mice serum and the pro-apoptotic factor caspase-3 in myocardium indicated that miR-17-5p inhibitor suppressed MI/R-induced death of cardiomyocytes ($p < 0.05$) (Fig. 1f and g). Moreover, the percentage of apoptotic cells evaluated by the TUNEL assay showed that MI/R caused an obvious increase of apoptosis

($p < 0.01$) compared with the sham group, which could be effectively diminished ($p < 0.05$) by miR-17-5p inhibitor (Fig. 1h).

Downregulation of miR-17-5p attenuated ER stress in myocardium during MI/R

After determining the role of miR-17-5p in MI/R-induced apoptosis of cardiomyocytes, we further evaluated if this function is related with ER stress. Bip, CHOP, and phosphorylation of PERK were regarded as biomarkers of enhanced ER stress. We observed elevated expression levels of Bip (Fig. 2a) and CHOP (Fig. 2b) in mice myocardium after MI/R compared with the sham group ($p < 0.05$), while miR-17-5p inhibitor injection markedly reduced this effect ($p < 0.05$). Western blotting results further demonstrated that the administration of miR-17-5p inhibitor significantly reversed the elevated expression levels of p-PERK, Bip, and CHOP ($p < 0.05$) in myocardium after MI/R (Fig. 2c).

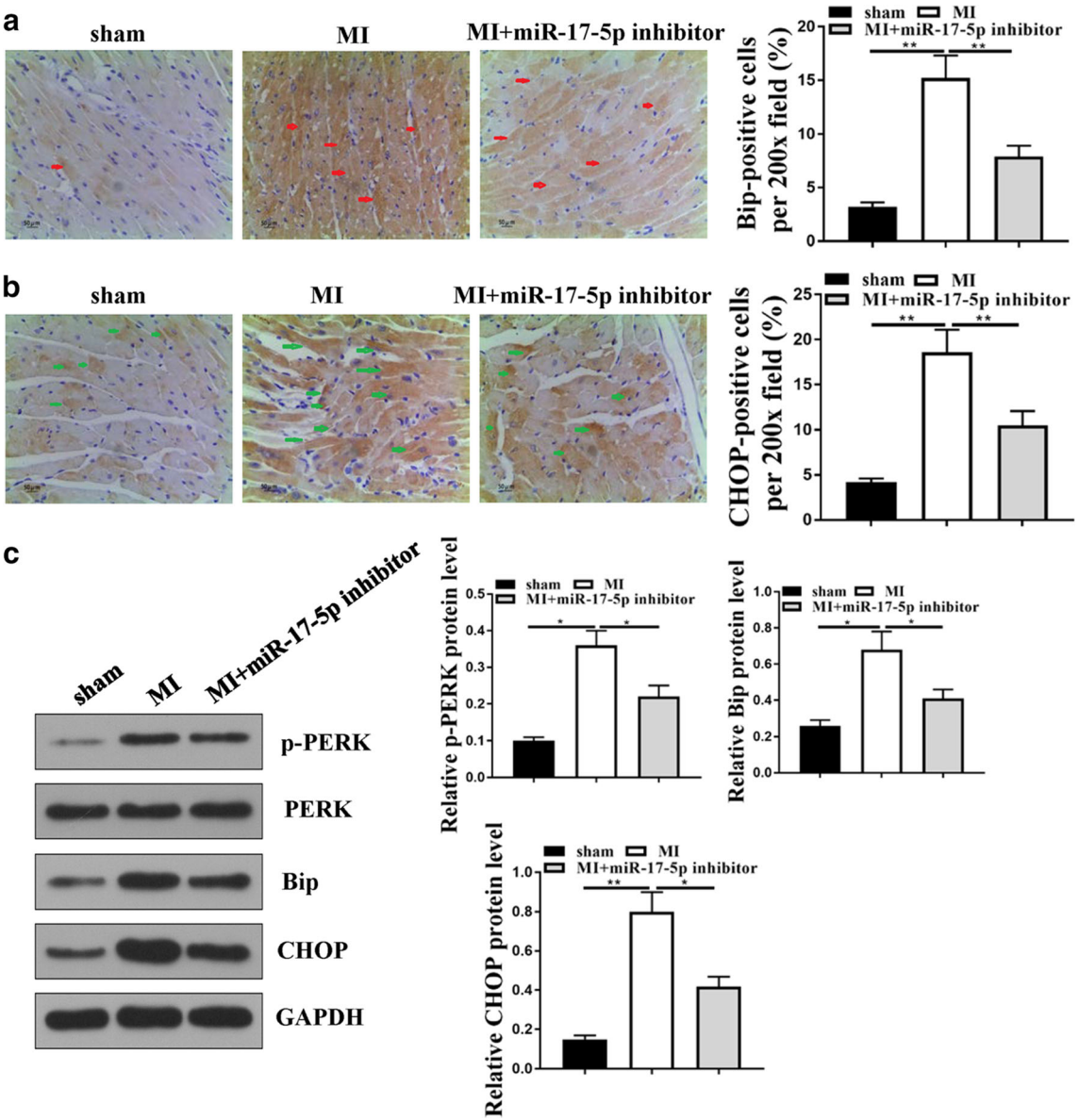

Fig. 2 Downregulation of miR-17-5p attenuated ER stress in myocardium during MI/R. **a**–**b** IHC assay for the detection of Bip (**a**) and CHOP (**b**) expression in mice myocardium after MI/R or combination with miR-17-5p inhibitor injection. The positive staining was calculated and shown in diagrams. Five random sections were captured and quantified for each sample. **c** Western blotting assay determined the protein levels of p-PERK, Bip, and CHOP in mice myocardium in the indicated group. Three independent experiments were repeated, $^{*}P < 0.05$, $^{**}P < 0.01$

Inhibition of ER stress attenuated the effect of miR-17-5p mimic in myocardium during MI/R

To confirm if miR-17-5p indeed affected the MI/R-induced heart injury via regulating ER stress signaling, we adopted the chemical agent 4-phenylbutyric acid (4-PBA), the inhibitor of ER stress response signaling, before injection of miR-17-5p mimics, to block ER stress-induced apoptosis, and established the MI/R mice model for 3 days. Then, we detected decreased EF ($p < 0.05$) (Fig. 3a) and FS ($p < 0.05$) (Fig. 3b) in mice hearts by echocardiography in mice injected with miR-17-5p mimic and a significant reverse ($p < 0.05$) in 4-PBA pretreatment group, indicating that blocking of ER stress response attenuated the effect of miR-17-5p during MI/R-induced myocardium injury. Additionally, miR-17-5p-promoted myocardium injury was indicated by elevated activity of LDH and caspase-3, and

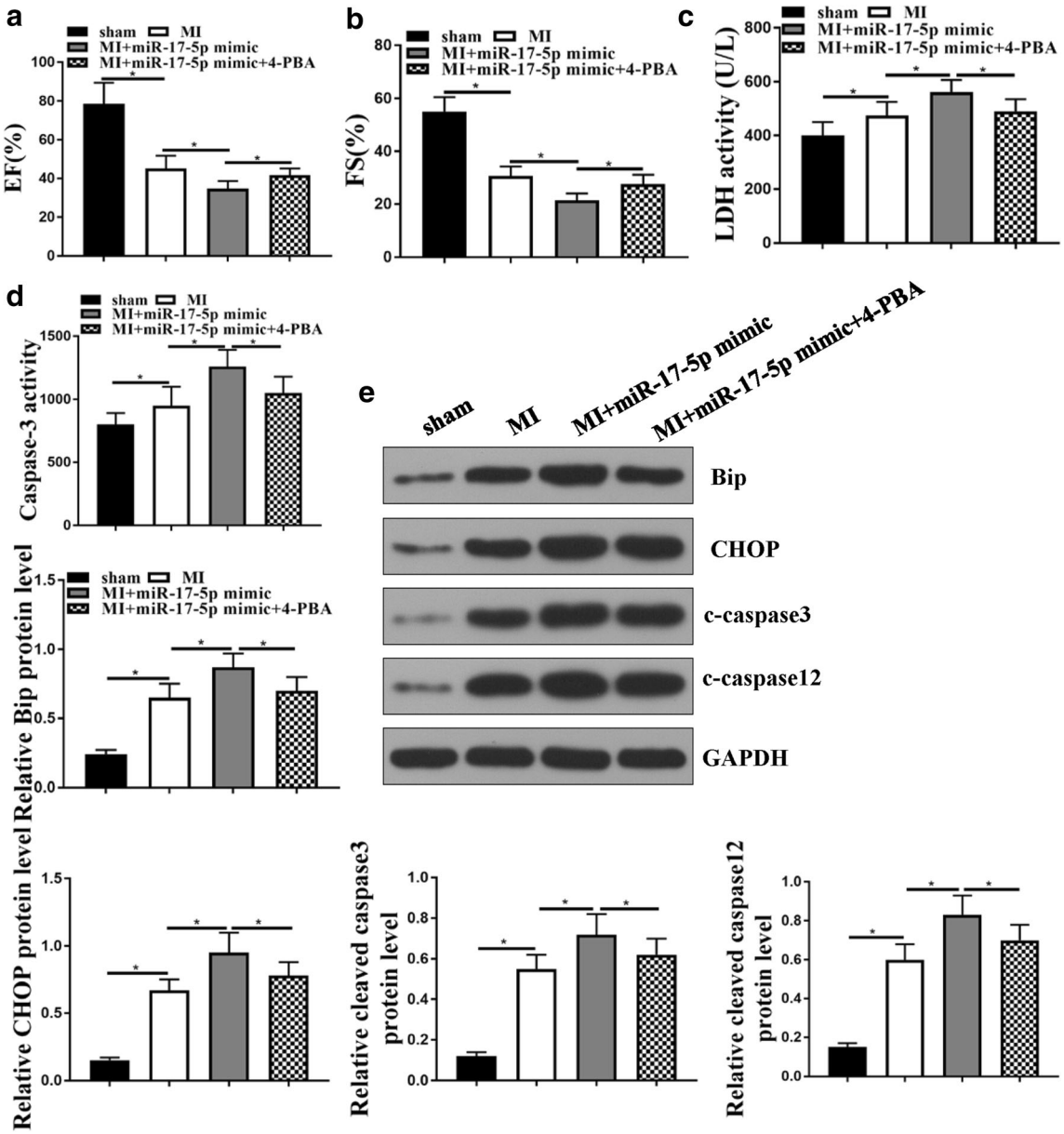

Fig. 3 Inhibition of ER stress by 4-PBA attenuates the effect of miR-17-5p mimic in myocardium during MI/R. **a–b** Echocardiography examination demonstrated the alteration of EF and FS in mice MI/R model under injection of miR-17-5p mimic and 4-PBA. Red arrow, Bip-positive staining; green arrow, CHOP-positive staining. **c–d** Serum level of LDH (**c**) and quantification of caspase-3 in myocardium (**d**) in mice MI/R model under injection of miR-17-5p mimic and 4-PBA. **e** Western blotting assay to determine the protein levels of Bip, CHOP, cleaved caspase-3, and caspase-12 in mice myocardium in the indicated group. The relative protein levels were shown in histograms. Three independent experiments were repeated, $^*P < 0.05$

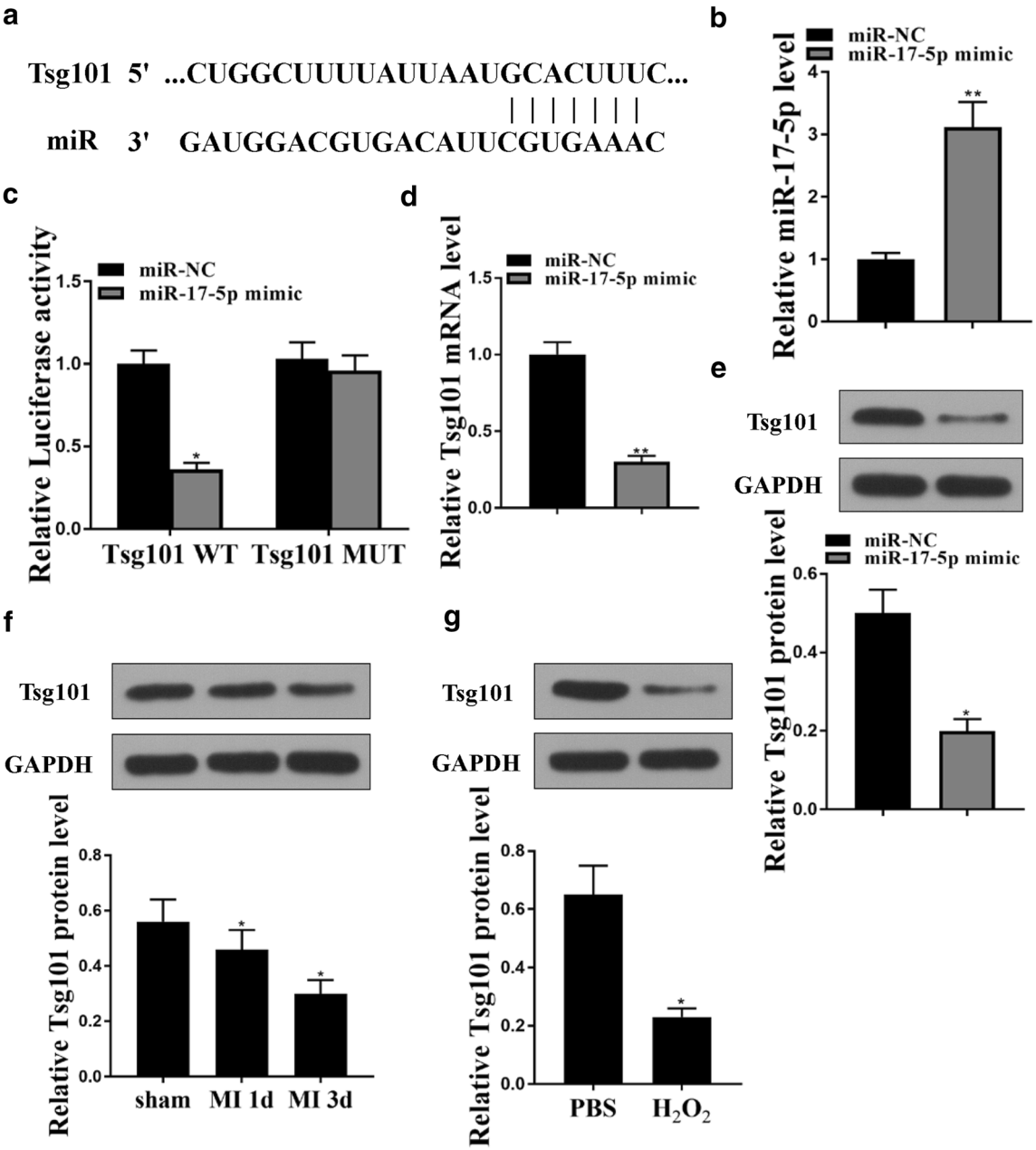

Fig. 4 MiR-17-5p targets Tsg101 in cardiomyocytes. **a** Bioinformatic prediction of interaction between miR-17-5p and Tsg101 mRNA. **b** QRT-PCR experiment detected the miR-17-5p level in H9c2 cells after transfection with miR-17-5p mimics. **c** 293T cells were transfected with miR-17-5p mimics along with pGL3-Tsg101-WT or pGL3-Tsg101-MUT, and luciferase activity was evaluated. **d–e** QRT-PCR and western blotting assay to detect the mRNA (**d**) and protein (**e**) levels of Tsg101 in H9c2 cells under transfection with miR-17-5p. **f** The expression of Tsg101 in myocardium after MI/R was detected by western blotting. **g** The expression of Tsg101 in H9c2 cells after H_2O_2 treatment for 4 h was detected by western blotting. The relative protein levels were shown in histograms. Three independent experiments were repeated, $^*P < 0.05$, $^{**}P < 0.01$ vs. NC, sham, or PBS

administration of 4-PBA could obviously impair this elevation ($p < 0.05$) (Fig. 3c and d). The expression and activation of ER stress response biomarkers Bip, CHOP, and caspase-12, as well as pro-apoptotic factor cleaved caspase-3, were upregulated ($p < 0.05$) in myocardium after treatment with MI/R and miR-17-5p mimic, and this effect was alleviated by 4-PBA ($p < 0.05$) (Fig. 3e), indicating the regulatory effect of miR-17-5p on ER stress response during MI/R.

Fig. 5 Tsg101 mediated the protective effects of miR-17-5p inhibitor in ▶ H_2O_2-induced H9c2 cells' injuries. **a** QRT-PCR experiment to determine the efficacy of shTsg101. **b** MTT assay to detect cell viability of H9c2 cells after treatment with H_2O_2, miR-17-5p inhibitor, or shTsg101. **c–d** Flow cytometry assay to detect cell apoptosis of H9c2 cells after treatment with H_2O_2, miR-17-5p inhibitor, or shTsg101. Apoptotic cells were calculated in histograms. **e** Western blotting assay to determine protein levels of Bip, CHOP, cleaved caspase-3, and cleaved caspase-12. The relative protein levels were quantified and shown in histograms. Three independent experiments were repeated, and the representative results were presented. $^*P < 0.05$, $^{**}P < 0.01$

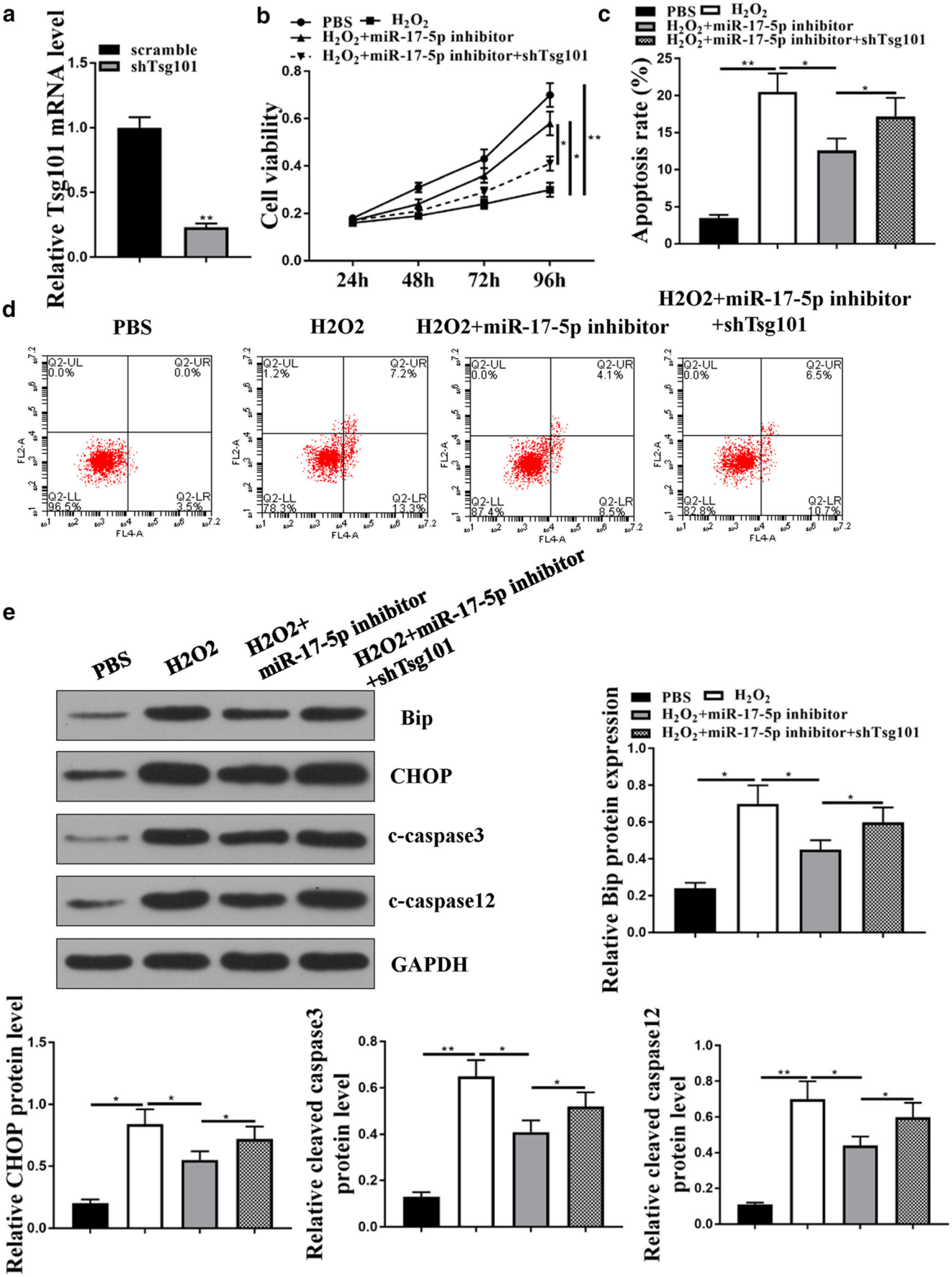
a
scramble
shTsg101
Relative Tsg101 mRNA level
b
PBS
H2O2
H2O2+miR-17-5p inhibitor
H2O2+miR-17-5p inhibitor+shTsg101
Cell viability
24h
48h
72h
96h
c
PBS
H2O2
H2O2+miR-17-5p inhibitor
H2O2+miR-17-5p inhibitor+shTsg101
Apoptosis rate (%)
d
PBS
H2O2
H2O2+miR-17-5p inhibitor
H2O2+miR-17-5p inhibitor +shTsg101
Q2-UL 0.0%
Q2-UR 0.0%
Q2-LL 96.5%
Q2-LR 3.5%
Q2-UL 1.2%
Q2-UR 7.2%
Q2-LL 78.3%
Q2-LR 13.3%
Q2-UL 0.0%
Q2-UR 4.1%
Q2-LL 87.4%
Q2-LR 8.5%
Q2-UL 0.0%
Q2-UR 6.5%
Q2-LL 82.8%
Q2-LR 10.7%
FL2-A
FL4-A
e
PBS
H2O2
H2O2+ miR-17-5p inhibitor
H2O2+miR-17-5p inhibitor +shTsg101
Bip
CHOP
c-caspase3
c-caspase12
GAPDH
Relative Bip protein expression
Relative CHOP protein level
Relative cleaved caspase3 protein level
Relative cleaved caspase12 protein level

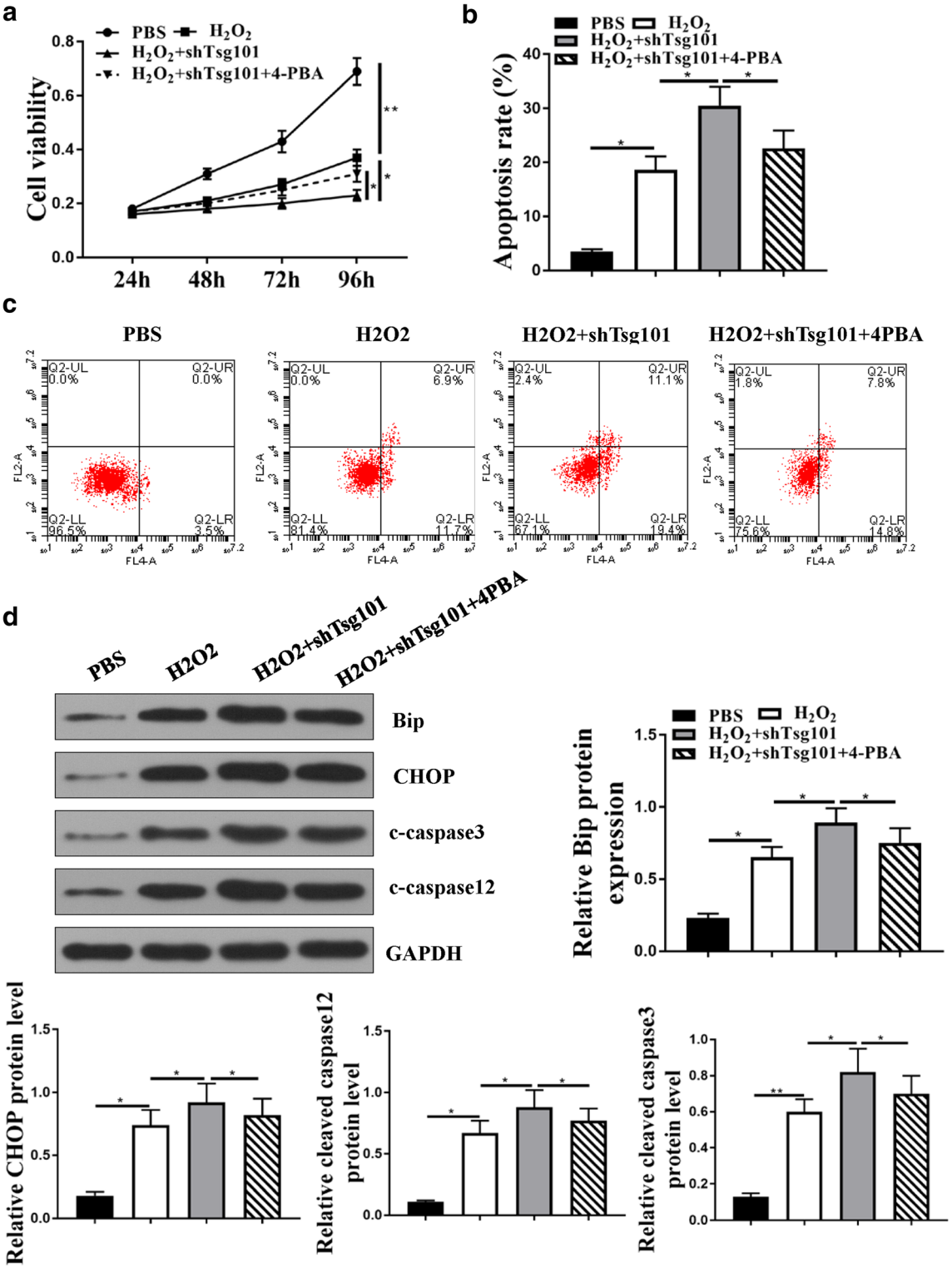

Fig. 6 Tsg101 participated in ER stress-mediated H9c2 cell injury. **a** MTT assay to detect cell viability of H9c2 cells after treatment with H_2O_2, shTsg101, and 4-PBA. **b–c** Flow cytometry assay to detect cell apoptosis of H9c2 cells after treatment with H_2O_2, shTsg101, and 4-PBA. Apoptotic cells were calculated in histograms. **d** Western blotting assay to determine protein levels of Bip, CHOP, cleaved caspase-3, and cleaved caspase-12. The relative protein levels were quantified and shown in histograms. Three independent experiments were repeated, and the representative results were presented. $^*P < 0.05$, $^{**}P < 0.01$

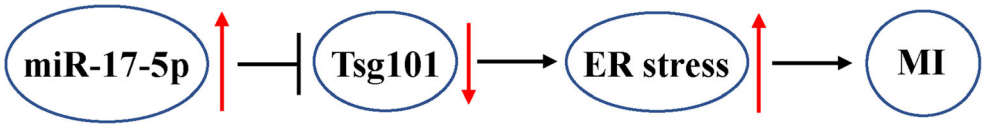

Fig. 7 Illustration of regulatory axis. MiR-17-5p downregulated the level of Tsg101 through targeting its 3′UTR region, subsequently activated ER stress and apoptosis of cardiomyocytes, and finally caused enhanced MI/R injury

MiR-17-5p targets Tsg101 in cardiomyocytes

The regulatory molecules involved in miR-17-5p regulated MI/R injury were then identified. Bioinformatic prediction indicated a putative binding site of miR-17-5p on Tsg101 mRNA (Fig. 4a). We conducted a transfection of miR-17-5p mimics to H9c2 and 293T cells to determine the interaction. A QRT-PCR experiment confirmed the efficacy of miR-17-5p mimics in H9c2 cells ($p < 0.15$) (Fig. 4b). A luciferase reporter assay revealed that co-transfection with miR-17-5p mimics reduced the activity of pGL3-Tsg101-WT ($p < 0.05$) but not pGL3-Tsg101-MUT, indicating the interaction of miR-17-5p with the wide-type Tsg101 but not the mutated Tsg101 (Fig. 4c). Transfection with miR-17-5p mimics significantly ($p < 0.01$) reduced the expression levels of Tsg101 in H9c2 cells at both the mRNA and protein levels (Fig. 4 d and e). Moreover, the expression levels of Tsg101 in mice myocardium declined markedly ($p < 0.05$) after MI/R (Fig. 4f). A similar reduction of Tsg101 ($p < 0.05$) was observed in apoptotic H9c2 cardiomyocytes after H_2O_2 treatment, compared with the control group (Fig. 4g). These results indicated that Tsg101 is a potential mediator in miR-17-5p regulated MI/R injury.

Tsg101 mediated the protective effects of miR-17-5p inhibitor in H_2O_2-induced H9c2 cells' injuries

We next conducted knockdown of Tsg101 to further investigate its role in miR-17-5p regulated apoptosis and ER stress response of cardiomyocytes. The efficacy of knockdown of shTsg101 was determined by qRT-PCR ($p < 0.05$) (Fig. 5a). The results of MTT and flow cytometry demonstrated that miR-17-5p inhibitor notably reversed the inhibited cell viability and elevated apoptosis induced by H_2O_2 treatment, while knockdown of Tsg101 markedly attenuated ($p < 0.01$) the recovered cell proliferation and impaired apoptosis caused by miR-17-5p inhibitor (Fig. 5b–d). Moreover, elevated levels of protein markers of ER stress-induced cell death, the Bip, CHOP, cleaved caspase-3, and cleaved caspase-12, were significantly suppressed by miR-17-5p inhibition ($p < 0.05$). However, knockdown of Tsg101 clearly disrupted the effects of miR-17-5p inhibitor ($p < 0.05$) (Fig. 5e). These results demonstrated the role of Tsg101 in miR-17-5p associated cell injury.

Tsg101 participated in ER stress-mediated H9c2 cell injury

After establishing the role of Tsg101 in miR-17-5p associated cell apoptosis of H9c2 in H_2O_2 treatment, we aimed to confirm that Tsg101 could regulate ER stress response by pretreatment of 4-PBA before knockdown of Tsg101 in a hypoxia-induced cardiomyocytes apoptosis model. MTT and flow cytometry were used to check cell proliferation and apoptosis. As shown in Fig. 6a, cell viability impaired by shTsg101 in H_2O_2 ($p < 0.01$) was alleviated ($p < 0.05$) by 4-PBA pretreatment (Fig. 6a). ER stress response blocked by 4-PBA also improved shTg101 enhanced cell apoptosis in an H_2O_2 hypoxia model ($p < 0.05$) (Fig. 6 b and c). Furthermore, although the biomarkers of ER stress-induced apoptosis, Bip, CHOP, cleaved caspase-3, and cleaved caspase-12, were significantly upregulated ($p < 0.05$) in the Tsg101 knockdown group compared with the control cells, 4-PBA treatment reversed these effects, which was consistent with the previous results (Fig. 6d). These results indicated that miR-17-5p/Tsg101 axis may affect MI/R injury via regulating ER stress response signaling.

To summarize the regulatory axis in this research, miR-17-5p downregulated the level of Tsg101 through targeting its 3′ UTR region, subsequently activating ER stress and apoptosis of cardiomyocytes, and finally causing enhanced MI/R injury (Fig. 7).

Discussion

Recent studies have demonstrated numerous novel strategies for the diagnosis and treatment of acute ischemia. The stability and easy detection in serum render microRNAs (miRNAs) promising targets in AMI research. MiRNAs mainly function through interacting with 3′ untranslated region (3′UTR) of the corresponding mRNA to disrupt the expression of target genes, which further leads to the alteration of critical regulatory factors in cellular physiological processes including cell proliferation, differentiation, autophagy, and apoptosis (Omidkhoda et al. 2019). Extensive studies have revealed the function of miRNAs in cardiovascular diseases, especially in myocardial ischemia. For example, miR-133, miR-21, miR-331, and miR-151 were shown to be elevated during myocardial infarction and were potential predictive and

diagnostic biomarkers for coronary artery disease (Horvath et al. 2020; Kaur et al. 2019; Kumar et al. 2020). MiR-26a-5p was reported to inhibit apoptosis of cardiomyocytes during ischemia reperfusion process by regulating PI3K/AKT pathway (Xing et al. 2020).

MiR-17-5p is a member of miRNA-17-92 cluster and participates in various pathological processes (Hao et al. 2017; Wang et al. 2019a; Xiao et al. 2019; Yu et al. 2010). Several studies have identified miR-17-5p as both an oncogenic factor and a tumor suppressor in several cancers (Yu et al. 2010; Zhang et al. 2007). In other diseases, the function of miR-17-5p also differs in various disease contexts. For example, it is reported to be associated with ischemia-induced cell death and to impair neuroprotection after cerebral ischemia injury via Smad signaling (Wang et al. 2019a). On the other hand, another study indicated that p53-induced miR-17-5p targets death receptor 6 to protect renal cells from ischemia/reperfusion injury (Hao et al. 2017). miRNA-17-92 cluster was also revealed to reduce ROS generation and to protect vascular endothelial HUVEC cells from cell death (Xiao et al. 2019). Thus, it is uncertain what role miR-17-5p plays during apoptosis of cardiomyocytes during AMI. In this study, we conducted a LAD operation to establish C57BL/6 mice MI/R model and H_2O_2-induced hypoxic H9c2 cardiomyocyte model to mimic human AMI. We revealed an elevated level of miR-17-5p on the first and third days after MI/R, and inhibition of miR-17-5p alleviated MI/R-induced heart injury and cardiomyocyte apoptosis. Here, we have determined the pro-apoptotic role of miR-17-5p during AMI and investigated the molecular mechanisms associated with this process.

Several studies have shown that pathological stress conditions such as oxidative stress, inflammatory stimulation, hypoxia, and ischemia disrupt the homeostasis of ER and lead to ER stress, caused by abnormal aggregation of unfolded and misfolded proteins. Additionally, it is widely recognized that ER stress leads to apoptosis of cardiomyocytes and further ischemia-related heart diseases (Glembotski 2007; Groenendyk et al. 2010; Li 2011; Logue et al. 2013). In normal cells, the UPR sensors PEPK, IRE1α, and ATF6 were maintained at an inactive state. When ER stress was elevated, such as with the accumulation of misfolded proteins, the homeostasis of ER was disrupted, and the status of BiP converted from attachment with UPR to dissociation, which induced the activation of PERK, IRE1α, and ATF6 via diverse mechanisms. For instance, the PERK protein initiated dimerization and autophosphorylation, which stimulated downstream protein translation-associated factor Eif2α and its phosphorylation and further enhanced the translation of ATF4 (activating transcription factor 4) (Vattem and Wek 2004). The elevation of ATF4 subsequently stimulated the transcriptional factor CHOP, which has been widely reported to participate in apoptosis and exert significant functions in ischemia (Chen et al. 2015; Nashine et al. 2014). It was reported that CHOP directly inhibited the anti-apoptotic protein Bcl2 and activated downstream caspase-12 cascade (Fu et al. 2010; Gaudette et al. 2014; McCullough et al. 2001). Meanwhile, inhibition of UPR by a chemical agent 4-phenylbutyric acid (4-PBA) exerted a notable protective effect on cardiomyocytes against myocardial ischemia, along with a significant reduction of CHOP levels (Luo et al. 2015). Thus, regulating the ER stress response could be a promising method of treating AMI. Considering the role of miR-17-5p in AMI-associated apoptosis and the profound impact of ER stress in AMI, we hypothesized whether miR-17-5p regulates ER stress response during AMI. The reduced levels of activated PERK, Bip, CHOP, caspase-3, and caspase-12 in MI/R heart tissues after miR-17-5p inhibition indicated the association between miR-17-5p and ER stress response. We further adopted the UPR inhibitor 4-PBA to block ER stress-induced apoptosis in a mice MI/R model. The echocardiography examination and detection of ER stress biomarkers demonstrated that attenuation of the ER stress response disrupted the myocardium injury induced by miR-17-5p mimics, which supported our hypothesis that miR-17-5p promoted myocardium injury via mediating the ER stress response. The specific mechanism of miR-17-5p regulation of ER is unclear. However, we found an impaired phosphorylation of PERK and decreased levels of Bip and CHOP under miR-17-5p inhibition. Thereby we hypothesized that miR-17-5p promoted the disassociation of Bip and subsequent phosphorylation of PERK stimulated the expression of CHOP, which further activated the apoptotic caspase signal and caused the death of cardiomyocytes.

Further bioinformatic prediction revealed Tsg101 as the potential target of miR-17-5p, and cellular experiments indicated a negative regulation of Tsg101 by miR-17-5p. Hence, we next examined the role of Tsg101 played in miR-17-5p-mediated ER stress response during MI/R. As previously reported in various studies, Tsg101 exhibited multiple functions on proliferation and differentiation of tumor cells, regulated cell cycle via p53 signaling and cyclin E1/CDK2 complex, and affected protein degradation signaling (Cheng and Cohen 2007; Goff et al. 2003; Xu and Zheng 2019). In our study, the knockdown of Tsg101 led to elevated levels of BiP and CHOP, which directly activated caspase-regulated cell apoptosis and exacerbated MI/R injury. However, the regulatory mechanism between Tsg101 and ER stress is not yet clear but may be associated with Tsg101-related protein degradation or other functions. We could discuss this regulatory axis in a further study. Detection of cell viability and ER stress-related apoptosis in an H_2O_2-induced H9c2 hypoxic model demonstrated that Tsg101 knockdown counteracted the protective effect of miR-17-5p inhibitor in a hypoxia model. Inhibition of the ER stress response by 4-PBA eliminated the effect of shTsg101, indicating that Tsg101 functions through mediating the ER stress response.

In conclusion, our study revealed an elevation of miR-17-5p during MI/R, presented a miR-17-5p/Tsg101 mediated ER

stress response and cardiomyocyte apoptosis during ischemia, and provided novel evidence for AMI treatment and diagnosis.

Funding Liaoning Natural Fund Guidance Program, No. 2019-ZD-0413.

Data availability The datasets used and/or analyzed during the current study are available from the corresponding author on reasonable request.

Compliance with ethical standards

Competing interests The authors declare that they have no competing interests.

Ethics approval and consent to participate All animal experiments in this study were approved according to the standards of Care and Use enacted by Laboratory Animals of The People's Hospital of Liaoning Province.

Consent for publication Not applicable.

Code availability Not applicable.

References

Chen BL, Sheu ML, Tsai KS, Lan KC, Guan SS, Wu CT, Chen LP, Hung KY, Huang JW, Chiang CK, Liu SH (2015) CCAAT-enhancer-binding protein homologous protein deficiency attenuates oxidative stress and renal ischemia-reperfusion injury. Antioxid Redox Signal 23:1233–1245. https://doi.org/10.1089/ars.2013.5768

Cheng TH, Cohen SN (2007) Human MDM2 isoforms translated differentially on constitutive versus p53-regulated transcripts have distinct functions in the p53/MDM2 and TSG101/MDM2 feedback control loops. Mol Cell Biol 27:111–119. https://doi.org/10.1128/MCB.00235-06

Chouchani ET et al (2014) Ischaemic accumulation of succinate controls reperfusion injury through mitochondrial ROS. Nature 515:431–435. https://doi.org/10.1038/nature13909

Choy KW, Murugan D, Mustafa MR (2018) Natural products targeting ER stress pathway for the treatment of cardiovascular diseases. Pharmacol Res 132:119–129. https://doi.org/10.1016/j.phrs.2018.04.013

Cunard R (2015) Endoplasmic reticulum stress in the diabetic kidney, the good, the bad and the ugly. J Clin Med 4:715–740. https://doi.org/10.3390/jcm4040715

Fu HY et al (2010) Ablation of C/EBP homologous protein attenuates endoplasmic reticulum-mediated apoptosis and cardiac dysfunction induced by pressure overload. Circulation 122:361–369. https://doi.org/10.1161/CIRCULATIONAHA.109.917914

Gaudette BT, Iwakoshi NN, Boise LH (2014) Bcl-xL protein protects from C/EBP homologous protein (CHOP)-dependent apoptosis during plasma cell differentiation. J Biol Chem 289:23629–23640. https://doi.org/10.1074/jbc.M114.569376

Glembotski CC (2007) Endoplasmic reticulum stress in the heart. Circ Res 101:975–984. https://doi.org/10.1161/circresaha.107.161273

Goff A, Ehrlich LS, Cohen SN, Carter CA (2003) Tsg101 control of human immunodeficiency virus type 1 Gag trafficking and release. J Virol 77:9173–9182. https://doi.org/10.1128/jvi.77.17.9173-9182.2003

Groenendyk J, Sreenivasaiah PK, Kim DH, Agellon LB, Michalak M (2010) Biology of endoplasmic reticulum stress in the heart. Circ Res 107:1185–1197. https://doi.org/10.1161/circresaha.110.227033

Hao J, Wei Q, Mei S, Li L, Su Y, Mei C, Dong Z (2017) Induction of microRNA-17-5p by p53 protects against renal ischemia-reperfusion injury by targeting death receptor 6. Kidney Int 91:106–118. https://doi.org/10.1016/j.kint.2016.07.017

Harisseh R, Abrial M, Chiari P, al-Mawla R, Villedieu C, Tessier N, Bidaux G, Ovize M, Gharib A (2019) A modified calcium retention capacity assay clarifies the roles of extra- and intracellular calcium pools in mitochondrial permeability transition pore opening. J Biol Chem 294:15282–15292. https://doi.org/10.1074/jbc.RA119.009477

Horvath M, Horvathova V, Hajek P, Stechovsky C, Honek J, Senolt L, Veselka J (2020) MicroRNA-331 and microRNA-151-3p as biomarkers in patients with ST-segment elevation myocardial infarction. Sci Rep 10:5845. https://doi.org/10.1038/s41598-020-62835-w

Karbasforooshan H, Roohbakhsh A, Karimi G (2018) SIRT1 and microRNAs: the role in breast, lung and prostate cancers. Exp Cell Res 367:1–6. https://doi.org/10.1016/j.yexcr.2018.03.023

Kaur A et al (2019) Systematic review of microRNA biomarkers in acute coronary syndrome and stable coronary artery disease. Cardiovasc Res. https://doi.org/10.1093/cvr/cvz302

Kumar D, Narang R, Sreenivas V, Rastogi V, Bhatia J, Saluja D, Srivastava K (2020) Circulatory miR-133b and miR-21 as novel biomarkers in early prediction and diagnosis of coronary artery disease. Genes (Basel) 11. https://doi.org/10.3390/genes11020164

Lazou A, Iliodromitis EK, Cieslak D, Voskarides K, Mousikos S, Bofilis E, Kremastinos DT (2006) Ischemic but not mechanical preconditioning attenuates ischemia/reperfusion induced myocardial apoptosis in anaesthetized rabbits: the role of Bcl-2 family proteins and ERK1/2. Apoptosis 11:2195–2204. https://doi.org/10.1007/s10495-006-0292-5

Li (2011) Involvement of endoplasmic reticulum stress-associated apoptosis in a heart failure model induced by chronic myocardial ischemia. Int J Mol Med 27. https://doi.org/10.3892/ijmm.2011.612

Logue SE, Cleary P, Saveljeva S, Samali A (2013) New directions in ER stress-induced cell death. Apoptosis 18:537–546. https://doi.org/10.1007/s10495-013-0818-6

Luo T, Kim JK, Chen B, Abdel-Latif A, Kitakaze M, Yan L (2015) Attenuation of ER stress prevents post-infarction-induced cardiac rupture and remodeling by modulating both cardiac apoptosis and fibrosis. Chem Biol Interact 225:90–98. https://doi.org/10.1016/j.cbi.2014.10.032

McCullough KD, Martindale JL, Klotz LO, Aw TY, Holbrook NJ (2001) Gadd153 sensitizes cells to endoplasmic reticulum stress by down-regulating Bcl2 and perturbing the cellular redox state. Mol Cell Biol 21:1249–1259. https://doi.org/10.1128/MCB.21.4.1249-1259.2001

McCully JD, Wakiyama H, Hsieh YJ, Jones M, Levitsky S (2004) Differential contribution of necrosis and apoptosis in myocardial ischemia-reperfusion injury. Am J Physiol Heart Circ Physiol 286:H1923–H1935. https://doi.org/10.1152/ajpheart.00935.2003

Miyazaki Y et al (2011) C/EBP homologous protein deficiency attenuates myocardial reperfusion injury by inhibiting myocardial apoptosis and inflammation. Arterioscler Thromb Vasc Biol 31:1124–1132. https://doi.org/10.1161/ATVBAHA.111.224519

Nakagawa T, Zhu H, Morishima N, Li E, Xu J, Yankner BA, Yuan J (2000) Caspase-12 mediates endoplasmic-reticulum-specific apoptosis and cytotoxicity by amyloid-beta. Nature 403:98–103. https://doi.org/10.1038/47513

Nashine S, Liu Y, Kim BJ, Clark AF, Pang IH (2014) Role of C/EBP homologous protein in retinal ganglion cell death after ischemia/reperfusion injury. Invest Ophthalmol Vis Sci 56:221–231. https://doi.org/10.1167/iovs.14-15447

Omidkhoda N, Wallace Hayes A, Reiter RJ, Karimi G (2019) The role of microRNAs on endoplasmic reticulum stress in myocardial

ischemia and cardiac hypertrophy. Pharmacol Res 150:104516. https://doi.org/10.1016/j.phrs.2019.104516

Rao RV, Ellerby HM, Bredesen DE (2004) Coupling endoplasmic reticulum stress to the cell death program. Cell Death Differ 11:372–380. https://doi.org/10.1038/sj.cdd.4401378

Rodriguez-Sinovas A, Abdallah Y, Piper HM, Garcia-Dorado D (2007) Reperfusion injury as a therapeutic challenge in patients with acute myocardial infarction. Heart Fail Rev 12:207–216. https://doi.org/10.1007/s10741-007-9039-9

Sai XB, Makiyama T, Sakane H, Horii Y, Hiraishi H, Shirataki H (2015) TSG101, a tumor susceptibility gene, bidirectionally modulates cell invasion through regulating MMP-9 mRNA expression. BMC Cancer 15:933. https://doi.org/10.1186/s12885-015-1942-1

Takakura S et al (2008) Oncogenic role of miR-17-92 cluster in anaplastic thyroid cancer cells. Cancer Sci 99:1147–1154. https://doi.org/10.1111/j.1349-7006.2008.00800.x

Urano F, Wang X, Bertolotti A, Zhang Y, Chung P, Harding HP, Ron D (2000) Coupling of stress in the ER to activation of JNK protein kinases by transmembrane protein kinase IRE1. Science 287:664–666. https://doi.org/10.1126/science.287.5453.664

Vattem KM, Wek RC (2004) Reinitiation involving upstream ORFs regulates ATF4 mRNA translation in mammalian cells. Proc Natl Acad Sci U S A 101:11269–11274. https://doi.org/10.1073/pnas.0400541101

Walter P, Ron D (2011) The unfolded protein response: from stress pathway to homeostatic regulation. Science 334:1081–1086. https://doi.org/10.1126/science.1209038

Wang M, Kaufman RJ (2016) Protein misfolding in the endoplasmic reticulum as a conduit to human disease. Nature 529:326–335. https://doi.org/10.1038/nature17041

Wang GK et al (2010) Circulating microRNA: a novel potential biomarker for early diagnosis of acute myocardial infarction in humans. Eur Heart J 31:659–666. https://doi.org/10.1093/eurheartj/ehq013

Wang JQ et al (2019a) Knockdown of microRNA-17-5p enhances the neuroprotective effect of Act A/Smads signal loop after ischemic injury. Neurochem Res 44:1807–1817. https://doi.org/10.1007/s11064-019-02815-3

Wang X et al (2019b) Crocin alleviates myocardial ischemia/reperfusion-induced endoplasmic reticulum stress via regulation of miR-34a/Sirt1/Nrf2. Pathway Shock 51:123–130. https://doi.org/10.1097/shk.0000000000001116

World Health Organization WHO | Cardiovascular diseases (CVDs) (2017) Available at: http://wwwwhoint/mediacentre/factsheets/fs317/en/

Xiao FJ et al (2019) miRNA-17-92 protects endothelial cells from erastin-induced ferroptosis through targeting the A20-ACSL4 axis. Biochem Biophys Res Commun 515:448–454. https://doi.org/10.1016/j.bbrc.2019.05.147

Xing X, Guo S, Zhang G, Liu Y, Bi S, Wang X, Lu Q (2020) miR-26a-5p protects against myocardial ischemia/reperfusion injury by regulating the PTEN/PI3K/AKT signaling pathway. Braz J Med Biol Res 53:e9106. https://doi.org/10.1590/1414-431X20199106

Xu C, Zheng J (2019) siRNA against TSG101 reduces proliferation and induces G0/G1 arrest in renal cell carcinoma – involvement of c-myc, cyclin E1, and CDK2. Cell Mol Biol Lett 24. https://doi.org/10.1186/s11658-018-0124-y

Yang S et al (2018) Downregulation of microRNA-17-5p improves cardiac function after myocardial infarction via attenuation of apoptosis in endothelial cells. Mol Gen Genomics 293:883–894. https://doi.org/10.1007/s00438-018-1426-5

Yu J, Ohuchida K, Mizumoto K, Fujita H, Nakata K, Tanaka M (2010) MicroRNA miR-17-5p is overexpressed in pancreatic cancer, associated with a poor prognosis, and involved in cancer cell proliferation and invasion. Cancer Biol Ther 10:748–757. https://doi.org/10.4161/cbt.10.8.13083

Zhang B, Pan X, Cobb GP, Anderson TA (2007) microRNAs as oncogenes and tumor suppressors. Dev Biol 302:1–12. https://doi.org/10.1016/j.ydbio.2006.08.028